Desalination and Water Treatment
www.deswater.com

doi: 10.5004/dwt.2019.23690

147 (2019) 222–233
April

Optimization of photocatalytic degradation of bisphenol A by novel Bi_2O_3–TiO_2 nano-composites under visible light irradiation

Nan Wang, Xing Li*, Yanling Yang, Tingting Guo, Xiaoxuan Zhuang, Siyang Ji, Tingting Zhang, Zhiwei Zhou*

College of Architecture and Civil engineering, Beijing University of Technology, Beijing 100124, China, Tel. +86 10 67391726; emails: lixing@bjut.edu.cn (X. Li), hubeizhouzhiwei@163.com (Z. Zhou), 15011163966@163.com (N. Wang), yangyanling@bjut.edu.cn (Y. Yang), gtyj914@163.com (T. Guo), zhuangxxuan@163.com (X. Zhuang), 489506654@qq.com (S. Ji), zhangting1229ztt@163.com (T. Zhang)

Received 15 May 2018; Accepted 24 December 2018

ABSTRACT

A series of Bi–Ti composited photocatalysts with different molar ratio of Bi/Ti (0.01:1(1%), 0.02:1(2%), 0.04:1(4%), and 0.05:1(5%)) and calcination temperature (400°C, 500°C, and 600°C) were prepared by sol-hydrothermal method. The properties of as-prepared photocatalysts were characterized by X-ray powder diffraction, scanning electron microscopy, transmission electron microscopy, X-ray photo-electron spectroscopy, Brunauer–Emmett–Teller, and ultraviolet–visible diffuse reflection spectroscopy. The selected photocatalyst (Bi-Ti-4%-600°C) was prepared under Bi/Ti molar ratio of 4% and calcination temperature of 600°C. Experimental variables during photocatalytic degradation were optimized for catalyst dosage, solution pH, initial bisphenol A (BPA) concentration, coexisting anions, and light source wavelength. Under optimal conditions of 1.0 g L^{-1} catalyst, pH 3, 30 mg L^{-1} initial BPA concentration, the degradation rate of BPA could reach up to 100% at 150 min under visible light irradiation. Compared with self-made pure TiO_2 and commercially available P_{25}, Bi-Ti-4%-600°C displayed an excellent photocatalytic activity for BPA degradation. Bi-Ti photocatalyst had a smaller crystal size, larger specific surface area, stronger visible light absorption ability, and lower band gap energy than self-made pure TiO_2. Four intermediates of BPA degradation were identified and a possible degradation pathway was proposed.

Keywords: Bi_2O_3–TiO_2 composites; Bisphenol A; Optimization; Degradation pathway

1. Introduction

Endocrine disrupting chemicals (EDCs), divided into four categories including natural compounds, pharmaceuticals, environmental pollutants, and chemicals related to industry, are emerging chemical contaminants that mimic or block the activity of natural hormones in humans and wildlife, thereby disrupting their reproductive system [1,2]. Several kinds of EDCs have been found in surface water, groundwater, runoff, landfill leachate, and even drinking water [3]. Bisphenol A (BPA), is widely used as an intermediate material for the production of polycarbonates, epoxy resins, and unsaturated polyester [4,5]. As a typical EDC, it suffers from many adverse effects, that is, brain development, sexual differentiation, behavior and immune function, and can continue to offspring, metabolic disorders in humans or animals [6,7]. Till now, researchers have developed various technologies to eliminate BPA in solution, such as biodegradation, sonochemistry, photochemistry, physical adsorption, and advanced oxidation process [8,9]. However, several problems, that is, high toxicity of intermediate products, high treatment cost, and low degradation efficiency,

* Corresponding authors.

have not been completely solved [10]. Therefore, efficient techniques for the decomposition and removal of BPA in water are required immediately.

Recently, using semiconductor photocatalysts to degrade pollutants has given rise to widespread attention [11]. Among various semiconductor photocatalysts, TiO_2-based photocatalysts are widely adopted due to their good chemical and thermal stability, non-toxicity, low cost, and high photocatalytic properties under UV irradiation [12]. However, due to the wide band gap, TiO_2 can only absorb UV light [13]. Exploiting novel and efficient photocatalyst, therefore, has been extensively urgent. Bismuth-based semiconductor photocatalysts, such as Bi_2WO_6, $Bi_2O_2CO_3$, Bi_2MoO_6, BiOX (X = I, Br, Cl), have attracted great attention recently, due to their high-efficiency visible-light response for the environmental treatment, and water splitting [14–17]. Many researchers have prepared photocatalysts of TiO_2 composited with Bi by sol-gel, hydrothermal, and emulsion electrospinning methods, such as Bi_2WO_6/TiO_2, $BiOCl/TiO_2$, $BiOI/TiO_2$, Bi_2S_3/TiO_2, $BiVO_4/TiO_2$, etc. [18–22]. The generation of heterogeneous structure by Bi oxide coupling TiO_2 can effectively expand the absorption of the visible light region and reduce the energy gap, which can form the electron–hole trapping, prolong the carrier lifetime, and inhibit the recombination of electron and hole, thereby enhancing the efficiency of photocatalytic degradation of pollutants under visible light irradiation [23,24].

In this study, a series of Bi_2O_3–TiO_2 nano-composites with different molar ratio of Bi/Ti (0.01:1(1%), 0.02:1(2%), 0.04:1(4%), and 0.05:1(5%)) and calcination temperature (400°C, 500°C, and 600°C) were prepared by sol-hydrothermal method. X-ray powder diffraction (XRD), scanning electron microscopy (SEM), transmission electron microscopy (TEM), X-ray photo-electron spectroscopy (XPS), Brunauer–Emmett–Teller (BET), and ultraviolet–visible diffuse reflection spectroscopy (UV-Vis DRS) was used to characterize the as-prepared composites. The photocatalytic degradation of BPA by Bi_2O_3–TiO_2 nano-composites under different variables, that is, catalyst dosage, solution pH, initial concentration of BPA, coexisting anions, and light source wavelength, were optimized. The degradation efficiency of selected Bi_2O_3–TiO_2 composite was evaluated compared with the pure TiO_2 and commercially available P_{25}. Stability of the selected Bi_2O_3–TiO_2 composite was also studied. Moreover, the intermediate products were identified, and a preliminary reaction pathway was proposed. The results of this study could provide an environmentally friendly Bi_2O_3–TiO_2 photocatalyst for efficient removal of BPA.

2. Materials and methods

2.1. Chemicals

BPA (>99.0%), bismuth nitrate pentahydrate ($Bi(NO_3)_3 \cdot 5H_2O$), tetrabutyl titanate, and sodium salt (NaCl, $NaHCO_3$, and Na_2SO_4) were purchased from Aladdin Industrial Corporation (Fengxian, Shanghai, China). Acetonitrile (HPLC grade) was obtained from Fisher Scientific (NJ, USA). All other reagents were purchased from Beijing Chemical Works (Beijing, China), and were all of analytical grade and used without further purification.

2.2. Preparation of Bi-Ti composites

The nano-composites of Bi-Ti-*a*-600°C and Bi-Ti-4%-*b* were prepared, where "*a*" and "*b*" represent the Bi/Ti molar ratio (1%, 2%, 4%, and 5%) and calcination temperature (400°C, 500°C, and 600°C), respectively. The Bi-Ti-*a*-600°C composites were prepared as follows: solution A was prepared by slowly pouring 10 mL tetrabutyl titanate (98.0 wt%) into 5 mL glacial acetic acid (99.0 wt%), subsequently the mixture was poured simultaneously into 40 mL anhydrous ethanol (99.7 wt%), and stirred by a magnetic mixer at 350 rpm for 120 min at room temperature. Solution B was prepared by dissolving a given amount of $Bi(NO_3)_3 \cdot 5H_2O$ in 50 mL deionized water under 40 kHz ultra-sonication for 30 min, and then stirred at 120 rpm by a magnetic mixer for 2 h. Solution B was added dropwise to solution A. The light-yellow transparent sol was obtained after mixing at 400 rpm for 5 h. The resulting sol was transferred into a Teflon recipient inside of stainless steel autoclave reactor. The hydrothermal treatment was conducted at 150°C for 12 h. The obtained precipitates were dried at 120°C and then calcined in air for 3 h at 600°C. For Bi-Ti-4%-*b* composites, the preparation procedures were the same as that of Bi-Ti-*a*-600°C, except that the Bi/Ti molar ratio was constantly kept at 4% and the calcination temperature changed from 400°C, 500°C to 600°C. The pure TiO_2 sample was also prepared by the same method as Bi-Ti-*a*-600°C without adding $Bi(NO_3)_3 \cdot 5H_2O$.

2.3. Experimental study

In the photocatalytic degradation experiment, a certain amount of photocatalyst was added into 250 mL BPA solution with different concentration in a cylindrical glass container which was surrounded by water cooling device. Subsequently, the samples were collected at different time intervals, and filtered through the BHLM syringe filters of size 0.22 μm. In the light source system for photocatalytic reaction, a 300 W Xe lamp (CEAULIGHT, CEL-HXF300E7) was set 12 cm above the surface of reaction solution. A 400 nm cut-off filter (UVIRCUT400) and reflectors (UVREF) were used to adjust the light of wavelength, which can obtain the visible light (400 nm < λ < 780 nm) and UV light (200 nm < λ < 400 nm). The visible light intensity was 280 mω cm^{-2} measured by a digital light power meter (CEL-NP2000-2). In order to study the effect of photolysis and catalysts adsorption of BPA, the control experiment was carried out without light source and catalyst. In addition, the photocatalytic efficiency of selected Bi-Ti composite was compared with pure TiO_2 and commercially available P_{25} (Degussa, Germany) under visible light irradiation.

2.4. Characterization of Bi-Ti nano-composites

The crystal phase composition of prepared Bi-Ti composites was determined by Rigaku SmartLab X-ray diffractometer using Cu-Kα radiation in the region 2Θ = 10°–80°. In order to study the surface composition and binding energy of samples, XPS (Quantera SXM, PHI, Japan) was used. The size, morphology, and microstructure of the as-prepared Bi-Ti composites was determined by HRTEM (JEM

2100F) and FE-SEM (SU-8010, Hitachi, Germany) with energy dispersive spectroscope (EDS). The UV-Vis DRS of Bi-Ti composites were measured using Hitachi U-3900 spectrometer. BET surface area and pores size distribution of the samples were measured by N_2 adsorption analyzer (TriStar II 3020M).

2.5. Analytic methods

BPA was analyzed by HPLC (1260 LC, Agilent, USA), in which C18 column (Waters, XBridge, 4.6 mm i.d. × 250 mm length, 5 μm) was employed. A UV-Vis detector was used and the detection wavelength for BPA was 278 nm. The mobile phase was ultrapure water/acetonitrile (50:50, v/v) and the flow rate was 1 mL min^{-1}.The mineralization degree was detected by a total carbon analyser vario TOC cube (Elementar, Germany). The intermediates produced during the BPA degradation were identified using a Q Exactive (Thermo Fisher) equipped with an electrospray ionization (ESI) source and operated in the positive (ESI+) and in the negative (ESI-) electrospray ionization mode. The spray voltage (+) was 3.5 kV, the spray voltage (–) was 3.2 kV, and capillary temperature was 320°C.

3. Results and discussion

3.1. Optimization of photocatalytic activity for BPA degradation

3.1.1. Effect of Bi/Ti molar ratio

The effect of Bi/Ti molar ratio (1%, 2%, 4%, and 5%) and calcination temperature (400°C, 500°C, and 600°C) of Bi-Ti composites on BPA degradation efficiency was investigated, the result is displayed in Fig. 1. As indicated, the degradation efficiency of BPA persistently increased as the reaction prolonged. When the Bi/Ti molar ratio was 4%, the photocatalytic degradation efficiency for BPA was the highest, reaching up to 88% (Fig. 1(a)). The calcination temperature of prepared Bi_2O_3–TiO_2 composites also played an important role in degrading BPA, more specifically, the degradation efficiency of BPA increased with the increase of calcination temperature (Fig. 1(b)). The higher calcination temperature rendered higher crystallinity and reduced the band gap, which made it more efficient to utilize photons and form electron–hole pairs, thus enhancing the photocatalytic effect [25]. In the following sections, we chose Bi-Ti-4%-600°C as an efficient composite, based on which the degradation rate of BPA of other experimental variables was further investigated.

3.1.2. Effect of Bi-Ti-4%-600°C dosage

The dosage of Bi_2O_3–TiO_2 composite (Bi-Ti-4%-600°C) on the degradation efficiency of BPA is displayed in Fig. 2. When the dosage of composite was 0.5 g L^{-1}, the degradation efficiency of BPA within 180 min was lower than that of 1.0 and 1.5 g L^{-1}. When the dosage increased up to 1.5 g L^{-1}, the increased turbidity of the solution led to the increase of light scattering, which was not conducive to the propagation of light. Thus, the photocatalytic degradation efficiency of 1.0 g L^{-1} was higher than that of 1.5 g L^{-1} within 90 min. Lower dosage of Bi-Ti-4%-600°C provided relatively few active sites, which ultimately affected the adsorption and degradation of BPA.

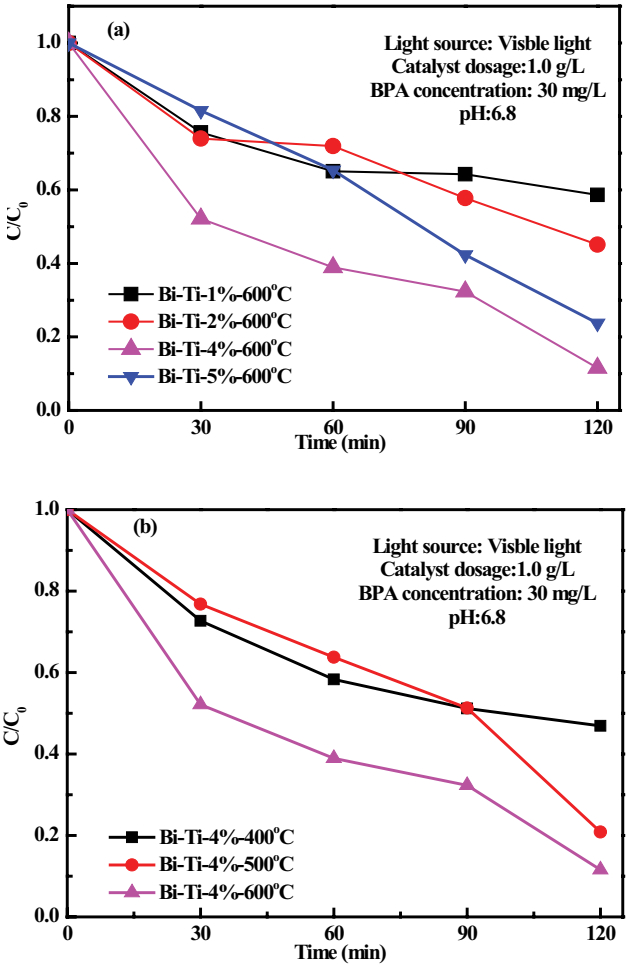

Fig. 1. Effect of Bi/Ti molar ratios (a) and calcination temperature (b).

3.1.3. Effect of solution pH

It can be seen from Fig. 3 that the degradation efficiency of BPA decreased with the increase of solution pH. When the solution pH was 3.0 or 6.8, the BPA degradation efficiency could both reach 100% when the reaction time surpassed 150 and 180 min, respectively. The higher the acidity was, the faster the degradation rate was. When the solution pH was 11, the ability of the catalyst surface to adsorb BPA was inhibited by the action of the electrostatic repulsion, leading to the decrease of the photocatalytic efficiency. It was reported that since the effect of protonation on the surface of TiO_2, the surface groups were positively charged, which promoted the effective separation of photo-generated electrons and holes, and improved the photocatalytic efficiency [26].

3.1.4. Effect of initial concentration of BPA

Fig. 4 shows the effect of different initial concentration of BPA on the photocatalytic degradation by Bi-Ti-4%-600°C composite. It is obvious that the photocatalytic degradation efficiency decreased with the increase of the initial concentration of BPA solution, due to the increase of intermediate products induced by the increase of the initial concentration

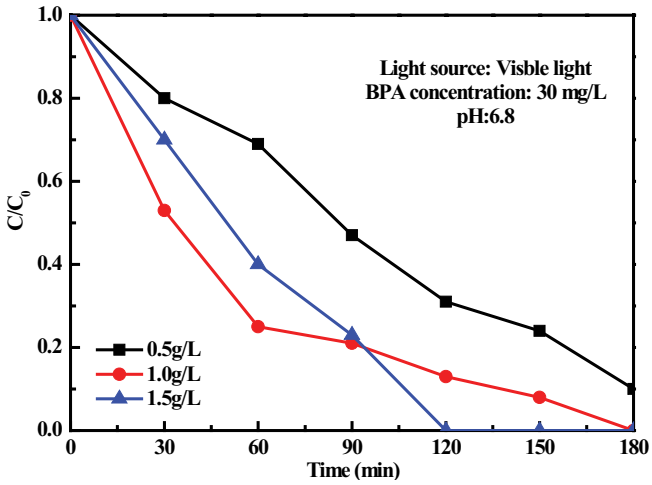

Fig. 2. Effect of Bi-Ti-4%-600°C composite dosage.

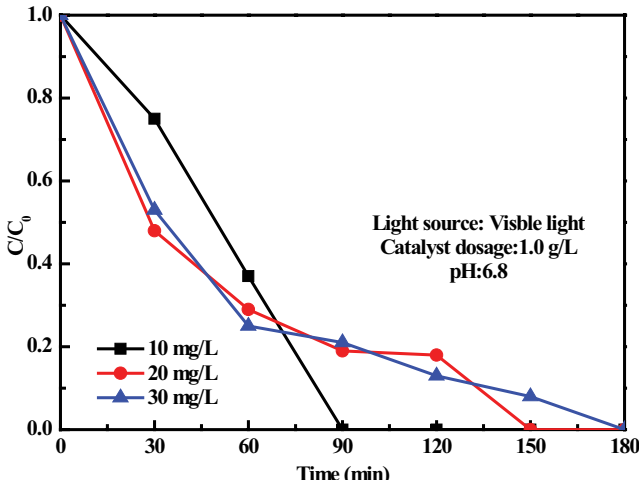

Fig. 4. Effect of initial concentration of BPA.

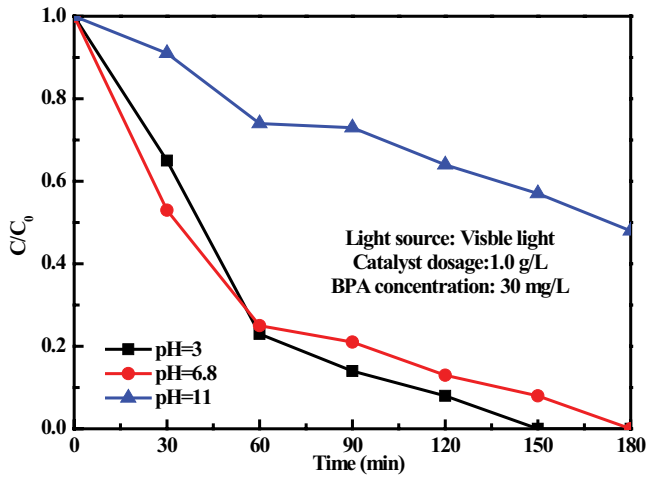

Fig. 3. Effect of solution pH.

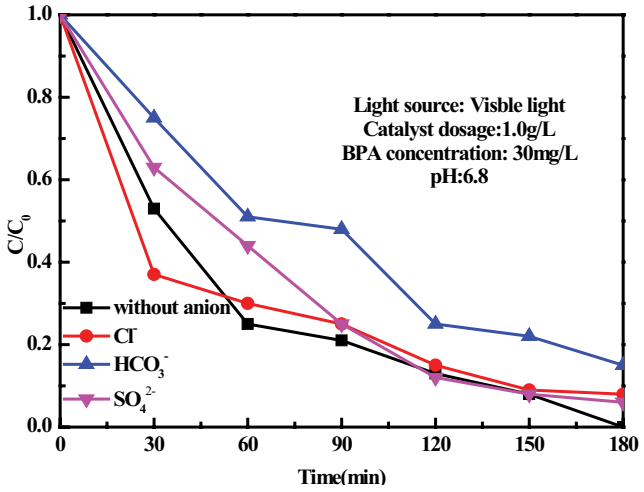

Fig. 5. Effect of inorganic anions.

of BPA. Since the number of intermediate products adsorbed onto the surface of the catalyst became larger, it inhibited the production of oxygen-containing active substances on the catalyst surface, resulting in the decreased photocatalytic efficiency of BPA [27].

3.1.5. Effect of inorganic anions

There are many inorganic anions in natural water, which coexist with organic pollutants. The presence of inorganic anions will affect the photocatalytic degradation of pollutants [28]. Fig. 5 shows the effect of the presence of inorganic anions in the solution on the BPA degradation efficiency. Three kinds of inorganic anions exerted inhibitory effect, and the inhibition degree was as following: HCO_3^- > Cl^- > SO_4^{2-}. As known, HCO_3^- is a free radical scavenger, which can directly quench of hydroxyl radicals on the catalyst surface. In addition, Cl^- and SO_4^{2-} can react with photogenerated holes on the catalyst surface to form free radicals with low oxidation activity, thereby reducing the efficiency of photocatalytic degradation of BPA.

3.1.6. Effect of light source wavelength

The wavelengths of the excited light source were adjusted to 200–400 nm, 400–780 nm, and all optical spectrum by using different kinds of filters. The effect of different light source wavelengths on the photocatalytic degradation of BPA is depicted in Fig. 6. Under the condition of solar spectrum, the BPA degradation efficiency was the highest, reaching up 100% at 60 min. While under the conditions of UV (200–400 nm) and visible light (400–780 nm), the degradation efficiency reached 100% at 90 and 180 min, respectively. It can be inferred that at relative low wavelength energy (400–780 nm), the photocatalytic degradation efficiency could be improved by prolonging illumination time. Therefore, the catalyst prepared in this study had broad spectrum applicability and high efficiency.

3.2. Comparison of prepared Bi-Ti-4%-600°C with other catalysts

BPA is a relative stable contaminant under visible light irradiation without catalyst as indicated in Fig. 7. In the absence of light irradiation, the curve of adsorption of

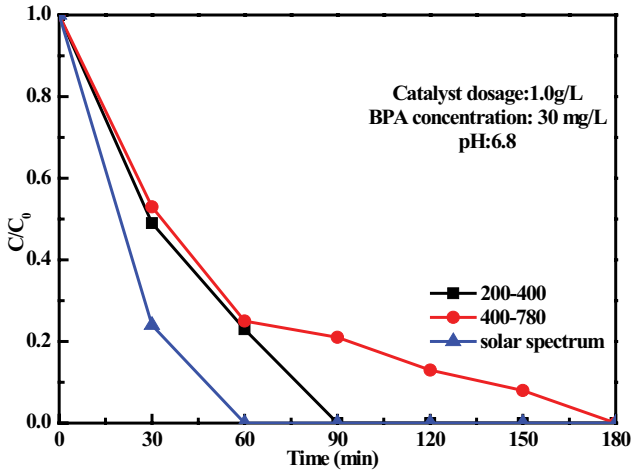

Fig. 6. Effect of light source wavelength.

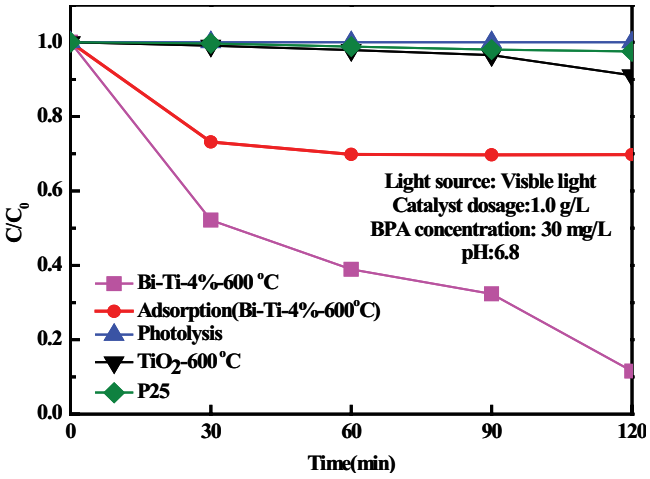

Fig. 7. Comparison of prepared Bi-Ti-4%-600°C with other catalysts.

Bi-Ti-4%-600°C reflected that the catalyst has an obvious adsorption and degradation effect on BPA within 30 min. When the reaction time was 60 min, the solution gradually reached the adsorption equilibrium. Under visible light irradiation, about 88% of BPA could be degraded by Bi-Ti-4%-600°C within 120 min, showing a superior catalytic reaction compared with P_{25} and self-made TiO_2. Therefore, Bi-Ti-4%-600°C could be used as photocatalysts to efficiently degrade BPA under visible light irradiation.

The comparison of as-prepared composite with TiO_2-based photocatalysts reported from other literatures for BPA degradation was made (Table 1).It was indicated that the Bi_2O_3–TiO_2 nano-composite prepared in this study was to the reported TiO_2-based photocatalysts under optimal conditions of visible light irradiation.

3.3. Characterization of the prepared Bi_2O_3–TiO_2 composites

3.3.1. XRD patterns of the prepared Bi-Ti-4%-600°C

The XRD patterns of self-made pure TiO_2 and Bi-Ti-4%-600°C are shown in Fig. 8. It was found that only anatase crystal phase presented in the Bi-Ti-4%-600°C. The diffraction peak of bismuth oxide was not observed due to the low content of bismuth. According to the XRD results, the average crystal size of the Bi-Ti-*a*-600°C composites was calculated by the Scherrer formula (Table 2). The particle size of Bi-Ti-*a*-600°C composites decreased significantly compared with TiO_2, which indicated that bismuth oxide in TiO_2 particles inhibited the crystal phase growth of TiO_2 during calcination process. Furthermore, peak intensities at 38.66° (112), 62.28° (213), and 76.25° (301) decreased and disappeared gradually. However, the particle sizes increased with the increase of Bi/Ti molar ratio, because of the newly formed Bi-O-Ti heterojunction interface between bismuth oxide and TiO_2 crystal. Crystal aggregation can be expected due to increased average particle size. Therefore, both the calcination temperature and Bi content influenced the particle size and crystallinity.

3.3.2. XPS of prepared Bi-Ti-4%-600°C

Fig. 9 shows the XPS of Bi-Ti-4%-600°C, it can be seen that the sample was composed of Ti, Bi, and O. As shown in Fig. 9(a), there were two strong peaks at 458.5 and 464.1 eV assigned to Ti $2p_{3/2}$ and Ti $2p_{1/2}$ in the high-resolution spectra, indicating that the valence state of Ti in Bi-Ti-4%-600°C was 4+, and there was no peak assigned to Ti^{3+} and Ti^{2+}. This finding was consistent with the result of Yap et al. [42]. In Fig. 9(b), the Bi $4f_{7/2}$ peak at 159.3 and Bi $4f_{5/2}$ peak at 164.7 eV revealed that the main valence of Bi was 3+ [43], corresponding with the value of pure Bi_2O_3 in other report [23,44]. The high resolution O 1s spectrum shown in Fig. 9(c) depicts peak at 529.6 eV, which belong to the oxygen of TiO_2 [45]. In summary, it could be inferred that the coexistence of Bi_2O_3 and TiO_2 in the heterostructure catalysts.

In combination with XRD and XPS analysis, it was found that Bi did not enter the TiO_2 lattice. When the amount of Bi doped was lower than the optimum value, the Bi-O-Ti heterogeneous crystal increased gradually with the increase of doped content. The formation of Bi-O-Ti crystal phase inhibited the lattice growth of TiO_2, resulting in the formation of a large surface area composite. As the content of Bi-O phase deposited on TiO_2 increased, carrier trapping traps were formed to promote separation of photo-generated electrons and holes, resulting in an enhanced photocatalytic effect. However, excess Bi-O could aggravate charges recombination process.

3.3.3. Morphology of prepared Bi-Ti-4%-600°C by SEM/TEM

As indicated in Fig. 10(a), uniform particle size of Bi-Ti-4%-600°C was observed, and the average diameter of such composite was about 12–13 nm, according to the TEM image in Fig. 10(b). The results were in agreement with the XRD analysis in Table 2. From the FE-SEM images in Fig. 10(c), it could be inferred that these particles were soft-agglomerates, which could be separated by ultra-sonication. EDS analysis in Fig. 10(d) also confirmed the presence of Bi, C, Ti, and O elements of Bi-Ti-4%-600°C composite, and the corresponding contents were 1.2, 9.2, 28.0, and 61.7 wt%, respectively.

Table 1
Comparison of as-prepared composite with reported TiO_2-based photocatalysts for BPA degradation

No	Catalyst	Preparation method	Reaction condition	BPA degradation efficiency	References
1	TiO_2/wood charcoal composites	Dip-sol-gel	UV irradiation, BPA concentration: 20 mg L^{-1}, catalyst dosage: 0.5 g L^{-1}, reaction time: 18 h	80.08%	[29]
2	N-F-TiO_2	Sol-gel	Visible irradiation, BPA concentration: 50 mg L^{-1}, catalyst dosage: 0.2 g L^{-1}, reaction time: 4 h	61.2%	[6]
3	TiO_2-MoS_2-RGO	Hydrothermal	UV irradiation, BPA concentration: 10 mg L^{-1}, catalyst dosage: 0.5 g L^{-1}, reaction time: 5 h	62.4%	[30]
4	Cu-TiO_2 nanorods	Microwave-assisted sol-gel/chemical reduction	UV and visible irradiation, BPA concentration: 10 mg L^{-1}, catalyst dosage: 1.0 g L^{-1}, reaction time: 2/3 h	Nearly 100%	[31]
5	CN-TiO_2	Solvothermal	UV irradiation, BPA concentration: 0.02 mg L^{-1}, catalyst dosage:0.5 g L^{-1}, reaction time:2 h	95%	[32]
6	TiO_2-RGO	Liquid-phase deposition	UV irradiation, BPA concentration: 10 mg L^{-1}, catalyst dosage: 0.5 g L^{-1}, reaction time: 15 min	95%	[11]
7	Ag_3PO_4/TiO_2	Not mentioned	Solar, UV and visible irradiation, BPA concentration: 220 μg L^{-1}, catalyst dosage: 0.25 g L^{-1}, reaction time: 2–3.5 min	100%	[33]
8	FeOOH/Fe_2O_3-TiO_2	Hydrothermal	Solar/visible irradiation, BPA concentration: 30/20 ppm, catalyst dosage: 0.1/1.0 g L^{-1}, reaction time: 1 h	About 50%	[34]
9	RGO/TiO_2/ZnO	Hydrothermal	UV/visible irradiation, BPA concentration: 10 mg L^{-1}, catalyst dosage: 0.5 g L^{-1}, reaction time: 3 h	99.7%/94.9%	[35]
10	F-TiO_2-RGO	Hydrothermal	UV irradiation, BPA concentration: 5 mg L^{-1}, catalyst dosage: 1.0 g L^{-1}, reaction time: 2 h	87.66%	[36]
11	N-B-TiO_2	Hydrothermal	Solar irradiation, BPA concentration: 1 μM, catalyst dosage: 0.4 g L^{-1}, reaction time: 2 h	100%	[37]
12	TiO_2/TNTs	Alkaline hydrothermal	UV irradiation, BPA concentration: 5 mg L^{-1}, catalyst dosage: 0.2 g L^{-1}, reaction time: 1 h	91.2%	[38]
13	TiO_{2-x}/rGO	Hydrothermal-calcination	Visible irradiation, BPA concentration: 2.5 mg L^{-1}, catalyst dosage: 1.0 g L^{-1}, reaction time: 1 h	91.0%	[39]
14	$ZnFe_2O_4$/TiO_2	Non-aqueous phase	Visible irradiation, BPA concentration: 10 mg L^{-1}, catalyst dosage: 1.0 g L^{-1}, reaction time: 30 min	90%	[40]
15	Ni-TiO_2	Microwave-assisted sol-gel	Visible irradiation, BPA concentration: 10 mg L^{-1}, catalyst dosage: 1.0 g L^{-1}, reaction time: 210 min	100%	[41]
16	Bi_2O_3–TiO_2	Sol-hydrothermal	Visible irradiation, BPA concentration: 30 mg L^{-1}, catalyst dosage: 1.0 g L^{-1}, pH 3.0, reaction time: 150 min	100%	This study

3.3.4. BET surface area analysis of prepared Bi-Ti-4%-600°C

The N_2 adsorption–desorption isotherms and pore distributions of Bi-Ti-4%-600°C are shown in Fig. 11. According to the IUPAC classification, the adsorption–desorption isotherms can be ascribed into type IV with hysteresis loops of type H1 at relative pressure of $0.7 < P/P_0 < 1.0$, indicating the mesoporous structure existed [46]. The specific surface area for Bi-Ti-4%-600°C was 69.7 $m^2 g^{-1}$ with mesopores ranging from 6.0 to 19.0 nm, along with pore volume of 0.255 $cm^3 g^{-1}$ and pore width of 12.4 nm, meanwhile the average pore width was about 14.3 nm. The formation of mesoporous structure of Bi-Ti-4%-600°C might be ascribed to the aggregation of particles, which could facilitate light scattering.

3.3.5. UV–Vis diffuse reflectance spectra of prepared Bi-Ti-4%-600°C

In order to clarify the energy band structure after Bi doping, UV-Vis DRS of Bi-Ti-4%-600°C sample is displayed in Fig. 12. Compared with pure TiO_2, a gradually red shift of the absorption spectra was observed after Bi doping with the increasing amount of Bi (Fig. 12(a)). The band gap of the

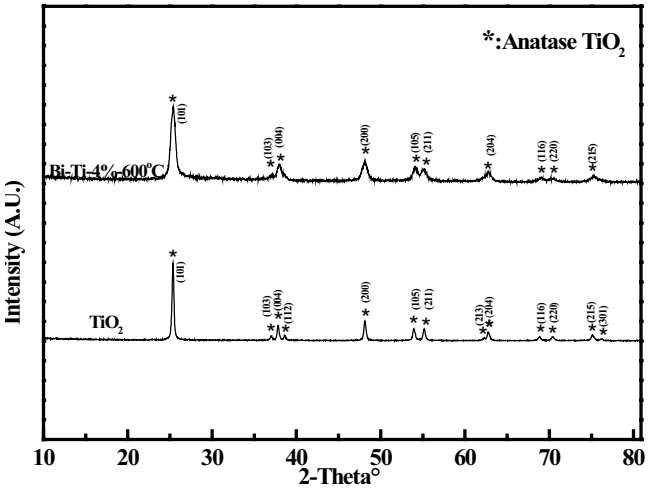

Fig. 8. XRD patterns of the prepared Bi-Ti-4%-600°C.

Bi-Ti-4%-600°C was 2.89 eV shown in Fig. 12(b), calculating from the plot of $[(\alpha h\nu)^{1/2}]$ vs. the photo energy ($h\nu$). The result showed that the Bi/Ti molar ratio had influenced on the band gap energy. Due to the different band edges of TiO_2 and Bi_2O_3, the potential difference was generated on the interface of the composite [23]. It can be expected that it is easier to transfer the photo-generated electrons and holes under visible light irradiation. Therefore, Bi-Ti-4%-600°C could effectively extend the absorption threshold of such composite to the visible light region.

3.4. Stability of Bi-Ti-4%-600°C during BPA photodegradation

The stability and reusability of Bi-Ti-4%-600°C was tested. At the end of each photocatalytic experiment, the selected Bi-Ti-4%-600°C was filtrated, washed, and dried at 70°C for 12 h to be prepared for the next use. Five photocatalytic experiment cycles were conducted. As shown in Fig. 13(a), the degradation efficiency of BPA after five cycles

Table 2
Physicochemical properties of the synthesized catalysts

Samples	TiO_2	Bi-Ti-1%-600	Bi-Ti-2%-600	Bi-Ti-4%-600	Bi-Ti-5%-600
Crystallite size[a] (nm)	41.4	11.6	12.8	13.0	15.9
Band gap energy[b] (eV)	3.07	3.02	2.97	2.89	2.90

[a]Determined from XRD patterns.
[b]Calculated using the Tauc plot method.

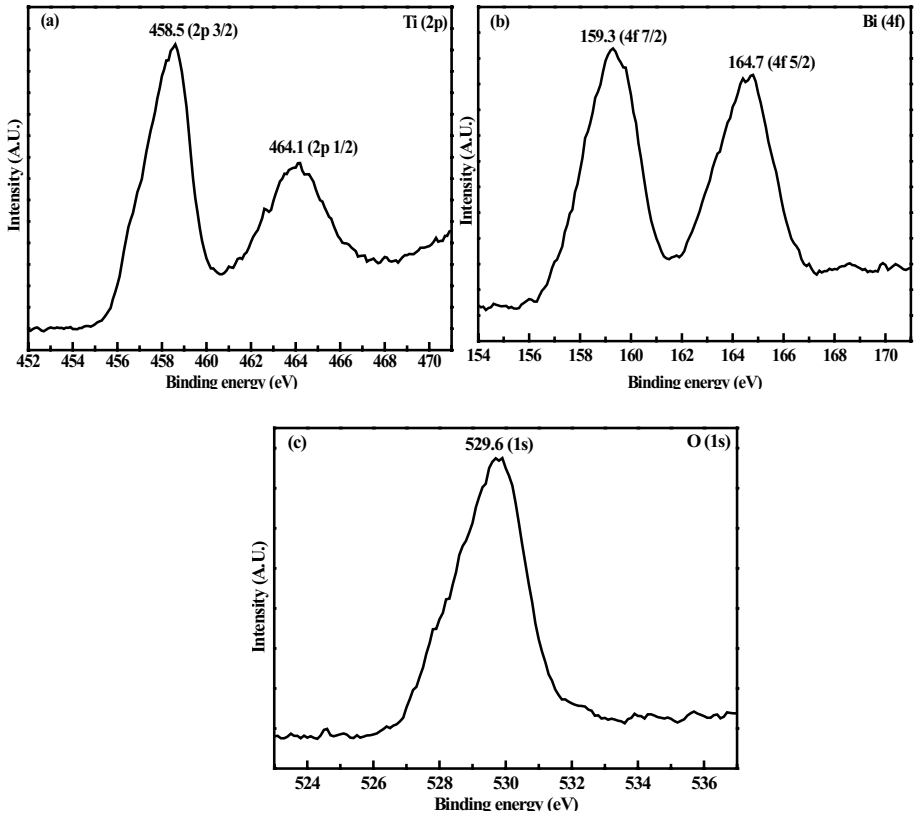

Fig. 9. High-resolution XPS spectra of Bi-Ti-4%-600°C. (a) Ti 2*p*, (b) Bi 4*f*, and (c) O 1*S*.

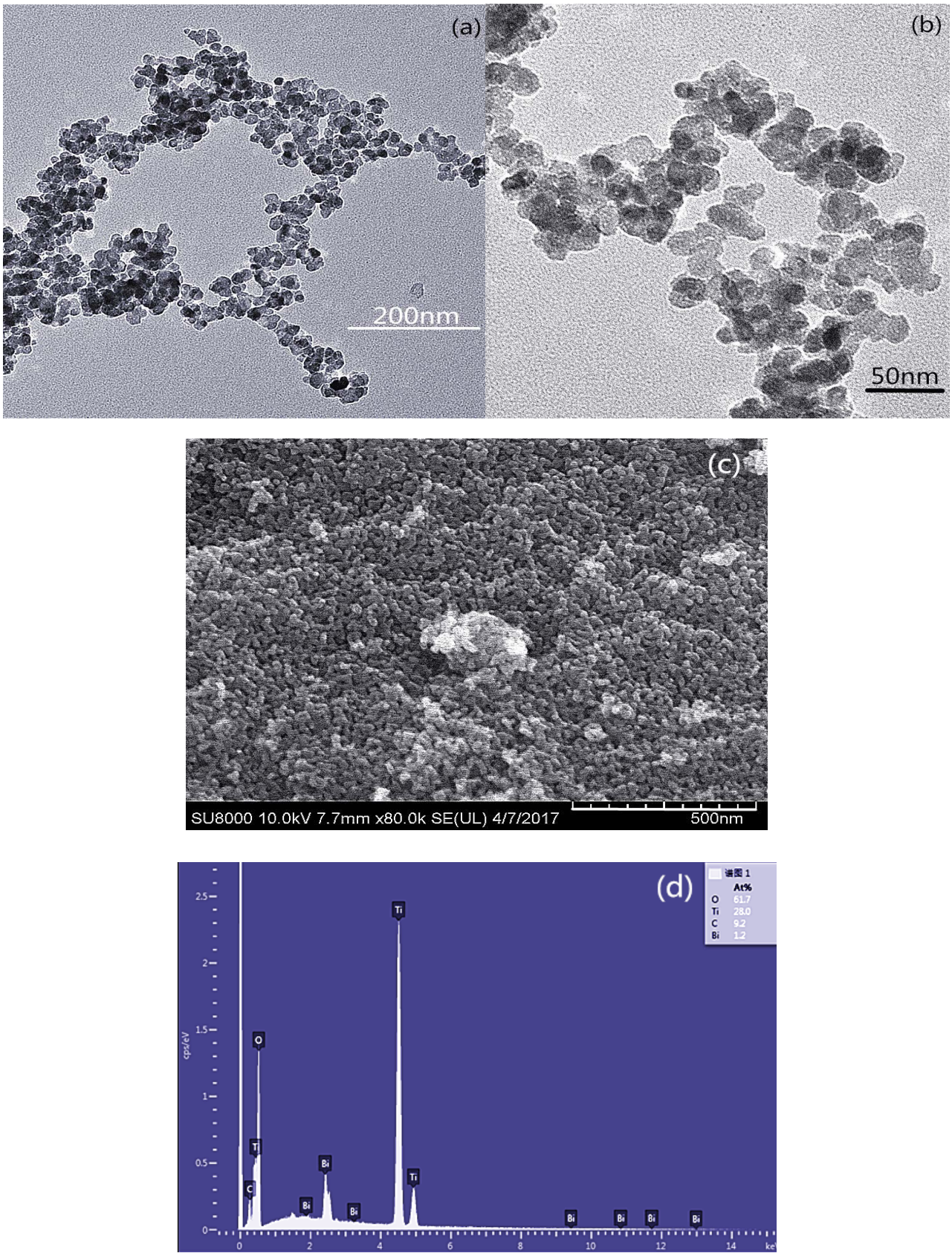

Fig. 10. TEM images (a) and (b), FESEM images (c), and EDS spectrum of Bi-Ti-4%-600°C (d).

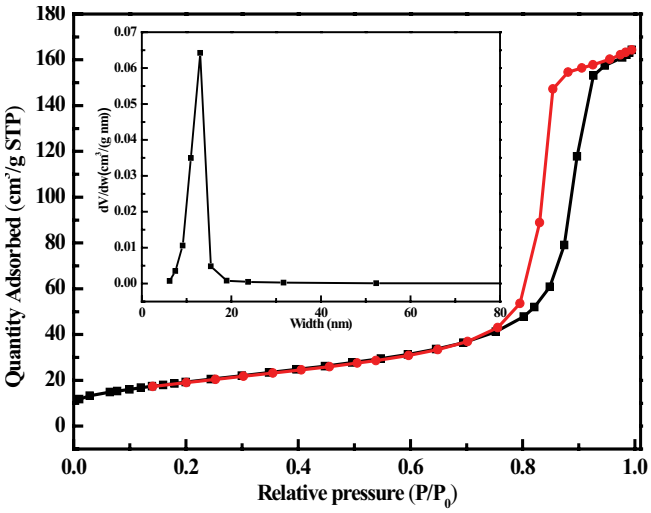

Fig. 11. N_2 adsorption–desorption isotherms of Bi-Ti-4%-600°C (inset: pore distribution).

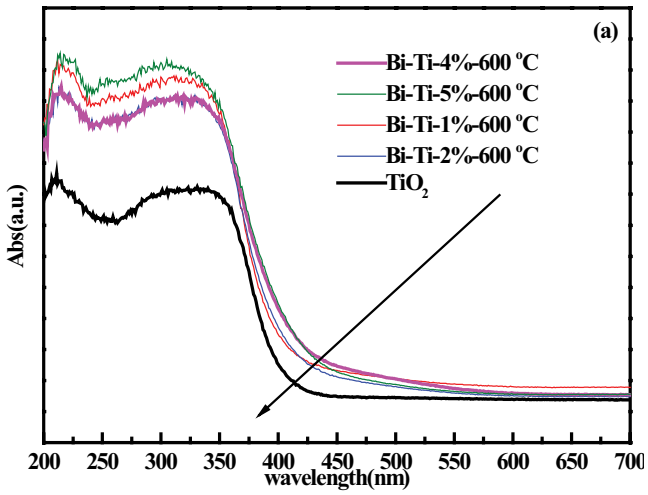

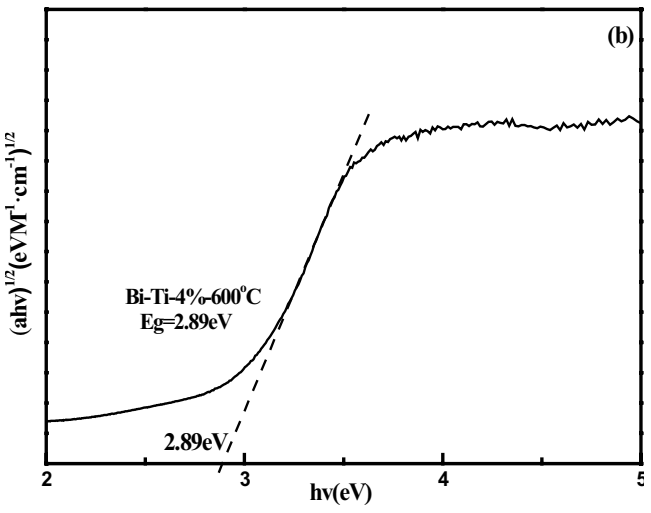

Fig. 12. UV-Vis spectra of prepared Bi-Ti-a-600°C composites (a), direct band gap of Bi-Ti-4%-600°C (b).

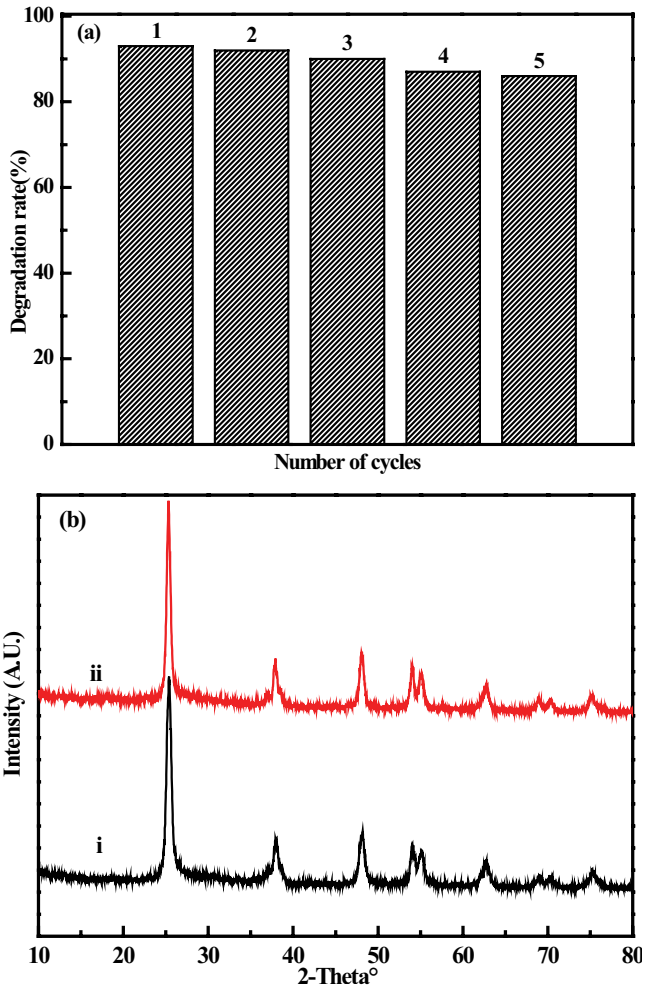

Fig. 13. Recycling of the Bi-Ti-4%-600°C composite (BPA solution concentration: 30 mg L^{-1}, 250 mL; catalyst dosage: 1.0 g L^{-1}; visible light irradiation for 180 min) (a), and XRD diffractograms of Bi-Ti-4%-600°C (i) before photocatalytic experiment, and (ii) after photocatalytic experiment) (b).

of reaction marginally decreased from 93% to 92%, 90%, 87%, and 86%, respectively. Because of the loss of Bi-Ti-4%-600°C in the washing and recycling process, the degradation rate decreased slightly. Barely no change of the XRD patterns was observed after cyclic degradation experiments (Fig. 13(b)), indicating its stability was good. Therefore, the photodegradation of BPA using Bi-Ti-4%-600°C was stable and recyclable.

3.5. Reactive species and possible mechanism

In order to explore the degradation mechanism of BPA by Bi-Ti-4%-600°C, the trapping test was conducted to determine the active species. Isopropyl alcohol (IPA) is usually used as a scavenger of·OH in the reaction, disodium ethylene diamine tetra acetate (EDTA) and benzoquinone (BQ) is used as scavengers of h^+ and $\cdot O_2^-$, respectively [47–49]. As shown in Fig. 14, the inhibition effect of the addition of IPA and BQ to photocatalytic degradation was obviously greater than that of EDTA, indicating that both ·OH and $\cdot O_2^-$ played dominant roles in photocatalytic degradation of BPA.

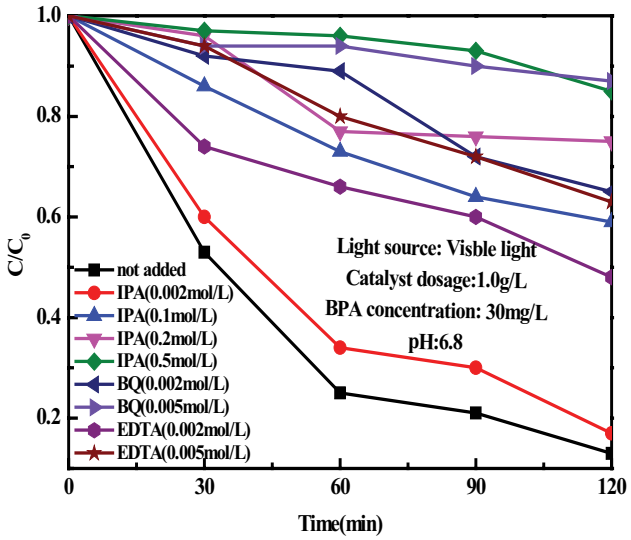

Fig. 14. Effect of reactive species on BPA degradation.

3.6. Mineralization and the degradation products/intermediates

Fig. 15(a) shows the mineralization of BPA during photocatalytic degradation by Bi-Ti-4%-600°C within 180 min, as measured by TOC concentration. The TOC decreased gradually with the increase of reaction time. When the reaction was 180 min, the degradation rate of TOC reached 75%.This phenomenon showed that the Bi-Ti-4%-600°C had a better mineralization of BPA. However, according to the previous research results, the removal efficiency of BPA could reach 100% when the visible light irradiated at 180 min. Therefore, the intermediate products were formed during photocatalytic degradation of BPA. The intermediate products formed during photocatalytic degradation at 180 min were identified as P_1, P_2, 4-isopropanolphenol, and hydroquinone. Table 3 lists the chemical formulas and fragments (m/z) of four intermediate products, of which 4-isopropanolphenol and hydroquinone were also found in other reports [27,50].

The possible BPA degradation pathway of Bi-Ti-4%-600°C was proposed (depicted in Fig. 15(b)). Specifically, first, the superoxide radicals ($\cdot O_2^-$) or hydroxyl radical (•OH) acted as the dominant active substance to attack the benzene ring of

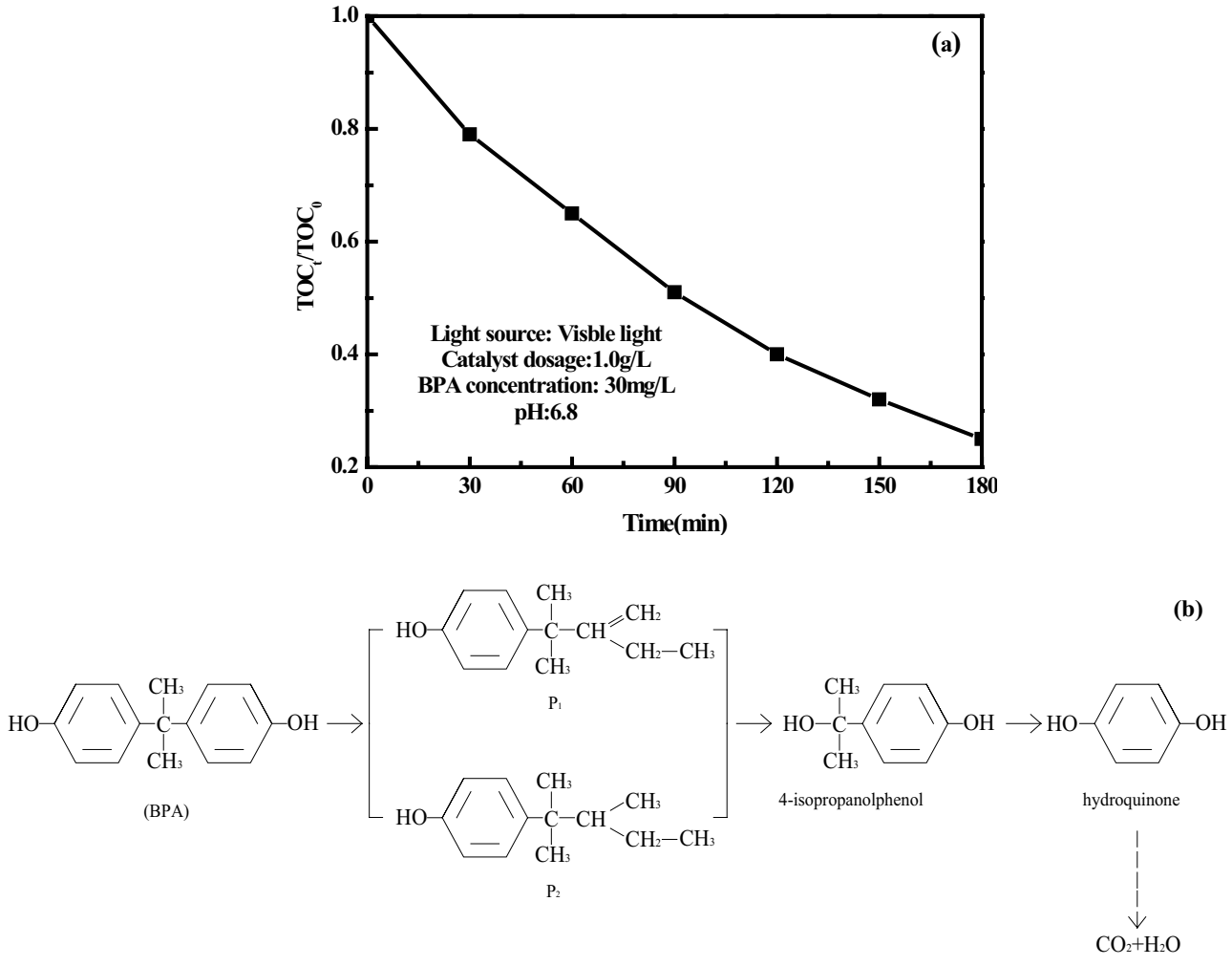

Fig. 15. Evolution of TOC during BPA photocatalytic degradation (a), proposed degradation pathways of BPA by Bi-Ti-4%-600°C (b).

Table 3
Chemical formulas and main fragments (m/z) of intermediate product

ID	*m/z*	Proposed structure
P_1	189	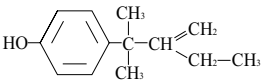
P_2	191	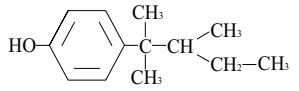
4-Isopropanolphenol	151	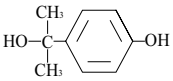
Hydroquinone	109	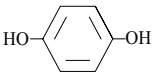

the BPA to form P_1 and P_2. Second, the methyl group was cracked to form 4-isopropanolphenol. It further converted into hydroquinone. These produced aromatic intermediates were oxidized aliphatic compounds, such as formic acid, acetic acid, and finally mineralized into CO_2 and H_2O through the ring rupture reaction [27,50,51].

4. Conclusion

A series of Bi_2O_3–TiO_2 composites were prepared by sol-hydrothermal method. The photocatalytic degradation of BPA of Bi_2O_3–TiO_2 composites was evaluated and optimized. The main conclusions of this work were as following:

- Bi-Ti photocatalyst with Bi/Ti molar ratio of 4% and the calcination temperature of 600°C displayed the best performance. Compared with self-made pure TiO_2 and commercially available P_{25}, Bi-Ti-4%-600°C displayed an excellent photocatalytic activity for BPA degradation. The prepared Bi-Ti-4%-600°C exhibited better crystallinity, smaller particle size, higher specific surface area, lower band gap energy and stronger visible light absorption capacity.
- Under the optimal conditions of catalyst dosage of 1.0 g L^{-1}, initial BPA concentration of 30 mg L^{-1}, pH 3, the degradation rate of Bi-Ti-4%-600°C reached 100% at 150 min under visible light irradiation.
- The intermediate products of P_1, P_2, 4-isopropanolphenol and hydroquinone were identified, the possible BPA degradation pathways were proposed.
- In our future research, we will prepare more novel materials by using Bi-Ti composites immobilized on the carbon-based adsorption medium, aiming to achieve a higher BPA removal efficiency through collaborations of photocatalytic activity and adsorption, in addition to the recovery of the nano-scale photocatalytic materials potentially.

Acknowledgements

The authors acknowledge the financial support of the National Natural Science Foundation of China (51778012). The authors would like to give their sincere thanks to the peer-reviewers for their suggestions.

References

[1] M. Gmurek, M. Olak-Kucharczyk, S. Ledakowicz, Photochemical decomposition of endocrine disrupting compounds – a review, Chem. Eng. J., 310 (2017) 437–456.
[2] T. Olmez-Hanci, I. Arslan-Alaton, B. Genc, Bisphenol a treatment by the hot persulfate process: oxidation products and acute toxicity, J. Hazard. Mater., 263 (2016) 283.
[3] A.F. Torovélez, C.A. Maderaparra, M.R. Peñavarón, W.Y. Lee, J.C. Bezares-Cruz, W.S. Walker, H. Cardenas-Henao, S. Quesada-Calderon, BPA and NP removal from municipal wastewater by tropical horizontal subsurface constructed wetlands, Sci. Total. Environ., 542 (2016) 93–101.
[4] A. Bhatnagar, I. Anastopoulos, Adsorptive removal of bisphenol A (BPA) from aqueous solution: a review, Chemosphere, 168 (2016) 885–902.
[5] S. Gao, C. Guo, J. Lv, Q. Wang, Y. Zhang, S. Hou, J. Gao, J. Xu, A novel 3D hollow magnetic Fe_3O_4/BiOI heterojunction with enhanced photocatalytic performance for bisphenol A degradation, Chem. Eng. J., 307 (2017) 1055–1065.
[6] X. He, W.G. Aker, M. Pelaez, Y. Lin, D. Dionysiou, H. Hwang, Assessment of nitrogen-fluorine-codoped TiO_2 under visible light for degradation of BPA: implication for field remediation, J. Photoch. Photobio. A, 314 (2016) 81–92.
[7] J. Rajasarkka, M. Pernica, J. Kuta, J. Lasnak, Z. Simek, L. Blaha, Drinking water contaminants from epoxy resin-coated pipes: a field study, Water Res., 103 (2016) 133–140.
[8] B. Cedat, C.D. Brauer, H. Metivier, N. Dumont, R. Tutundjan, Are UV photolysis and UV/H_2O_2 process efficient to treat estrogens in waters? Chemical and biological assessment at pilot scale, Water Res., 100 (2016) 357–366.
[9] J.R. Koduru, L.P. Lingamdinne, J. Singh, K. Choo, Effective removal of bisphenol A (BPA) from water using a goethite/activated carbon composite, Process Saf. Environ., 103 (2016) 87–96.
[10] Y. Chen, K. Liu, Fabrication of magnetically recyclable Ce/N co-doped TiO_2/$NiFe_2O_4$/diatomite ternary hybrid: improved photocatalytic efficiency under visible light irradiation, J. Alloys Compd., 697 (2017) 161–173.
[11] G. Liao, D. Zhu, J. Zheng, J. Yin, B. Lan, L. Li, Efficient mineralization of bisphenol A by photocatalytic ozonation with TiO_2-graphene hybrid, J. Taiwan Inst. Chem. Eng., 67 (2016) 300–305.
[12] W. Wu, G.Q. Shan, S.F. Wang, Environmentally relevant impacts of nano-TiO_2 on abiotic degradation of bisphenol A under sunlight irradiation, Environ. Pollut., 216 (2016) 166–172.
[13] V.A. Tran, T.T. Truong, T.A.P. Phan, T.N. Nguyen, T.V. Huynh, A. Agresti, S. Pescetelli, T.K. Le, A.D. Carlo, T. Lund, S. Le, P.T. Nguyen, Application of nitrogen-doped TiO_2 nano-tubes in dye-sensitized solar cells, Appl. Surf. Sci., 399 (2017) 515–522.
[14] Y. Lu, K. Zhao, Y.H. Zhao, S. Zhu, X. Yuan, M. Huo, Y. Zhang, Y. Qiu, Bi2WO6/TiO2/Pt nanojunction system: A UV-vis light responsive photocatalyst with high photocatalytic performance, Colloid. Surface. A, 481 (2015) 252–260.
[15] F. Duo, Y. Wang, C. Fan, X. Mao, X. Zhang, Y. Wang, J. Liu, Low temperature one-step synthesis of rutile TiO_2/BiOCl composites with enhanced photocatalytic activity, Mater. Charact., 99 (2015) 8–16.
[16] D. Wu, H. Wang, C. Li, J. Xia, X. Song, W. Huang, Photocatalytic self-cleaning properties of cotton fabrics functionalized with p-BiOI/n-TiO_2 heterojunction, Surf. Coat. Technol., 258 (2014) 672–676.
[17] S. Kumar, S. Sharma, S. Sood, A. Umar, S. Kansal, Bismuth Sulphide (Bi_2S_3) nanotubes decorated TiO_2 nanoparticles heterojunction assembly for enhanced solar light driven photocatalytic activity, Ceram. Int., 42 (2016) 17551–17557.
[18] J. Zhang, L. Huang, L. Yang, Z. Lu, X. Wang, G. Xu, E. Zhang, H. Wang, Z. Kong, J. Xi, Z. Ji, Controllable synthesis of Bi_2WO_6 (001)/TiO_2 (001) heterostructure with enhanced photocatalytic activity, J. Alloys Compd., 676 (2016) 37–45.

[19] K. Wang, C. Shao, X. Li, X. Zhang, N. Lu, F. Miao, Y. Liu, Hierarchical heterostructures of p-type BiOCl nanosheets on electrospun n-type TiO_2 nanofibers with enhanced photocatalytic activity, Catal. Commun., 67 (2015) 6–10.
[20] G.Q. Zhang, S. Ji, Y. Zhang, Y. Wei, Facile synthesis of p-n heterojunction of phosphorus doped TiO_2, and BiOI with enhanced visible-light photocatalytic activity, Solid State Commun., 259 (2017) 34–39.
[21] S. Boumaza, B. Bellal, A. Boudjemaa, M. Trari, Photodegradation of orange G by the hetero-junction x% Bi_2S_3 /TiO_2, under solar light, Sol. Energy, 139 (2016) 444–451.
[22] X.D. Zhu, F. Zhang, M.J. Wang, X. Gao, Y. Luo, J. Xue, Y. Zhang, J. Ding, S. Sun, J. Bao, C. Gao, A shuriken-shaped m-$BiVO_4$/{001}-TiO_2 heterojunction: synthesis, structure and enhanced visible light photocatalytic activity, Appl. Catal., A, 521 (2016) 42–49.
[23] S. Sood, S.K. Mehta, A.S.K. Sinha, S.K. Kansai, Bi_2O_3/TiO_2 heterostructures: synthesis, characterization and their application in solar light mediated photocatalysed degradation of an antibiotic, ofloxacin, Chem. Eng. J., 290 (2016) 45–52.
[24] E. Grabowska, M. Marchelek, T. Klimczuk, G. Trykowski, A. Zaleska-Medynska, Noble metal modified TiO_2, microspheres: surface properties and photocatalytic activity under UV-vis and visible light, J. Mol. Catal. A: Chem., 423 (2016) 191–206.
[25] Y. Hu, Y. Cao, P. Wang, D. Li, W. Chen, Y. He, X. Fu, Y. Shao, Y. Zheng, A new perspective for effect of Bi on the photocatalytic activity of Bi-doped TiO_2, Appl. Catal., B, 125 (2012) 294–303.
[26] P.S. Yap, T.T. Lim, M. Lim, M. Srinivasan, Synthesis and characterization of nitrogen-doped TiO_2/AC composite for the adsorption–photocatalytic degradation of aqueous bisphenol-A using solar light, Catal. Today, 151 (2010) 8–13.
[27] N. Lu, Y. Lu, F. Liu, K. Zhao, X. Yuan, Y. Zhao, Y. Li, H. Qin, J. Zhu, $H_3PW_{12}O_{40}$/TiO_2 catalyst-induced photodegradation of bisphenol A (BPA): kinetics, toxicity and degradation pathways, Chemosphere, 91 (2013) 1266–1272.
[28] B.F. GAO, P.S. Yap, T.M. Lim, T. Lim, Adsorption-photocatalytic degradation of Acid Red 88 by supported TiO_2: effect of activated carbon support and aqueous anions, Chem. Eng. J., 171 (2011) 1098–1107.
[29] L. Luo, Y. Yang, M. Xiao, L. Bian, B. Yuan, Y. Liu, F. Jiang, X. Pan, A novel biotemplated synthesis of TiO_2/wood charcoal composites for synergistic removal of bisphenol A by adsorption and photocatalytic degradation, Chem. Eng. J., 262 (2015) 1275–1283.
[30] L. Luo, J. Li, J. Dai, L. Xia, C. J. Barrow, H. Wang, J. Jegatheesan, M. Yang, Bisphenol A removal on TiO_2-MoS_2-reduced graphene oxide composite by adsorption and photocatalysis, Process Saf. Environ., 112 (2017) 274–279.
[31] L.F. Chiang, R. Doong, Cu-TiO_2 nanorods with enhanced ultraviolet- and visible-light photoactivity for bisphenol A degradation, J. Hazard. Mater, 277 (2014) 84–92.
[32] X. Wang, T.T. Lim, Effect of hexamethylenetetramine on the visible-light photocatalytic activity of C-N codoped TiO_2 for bisphenol A degradation: evaluation of photocatalytic mechanism and solution toxicity, Appl. Catal., A, 399 (2011) 233–241.
[33] M.E. Taheri, A. Petala, Z. Frontistis, D. Mantzavinos, D.I. Kondarides, Fast photocatalytic degradation of bisphenol A by Ag_3PO_4/TiO_2 composites under solar radiation, Catal. Today, 280 (2017) 99–107.
[34] G. Bao, H. Zhao, J. Chen, W. Deng, B. Jung, A. Abdel-Wahab, B. Batchelor, Y. Li, FeOOH and Fe_2O_3 co-grafted TiO_2 photocatalysts for bisphenol A degradation in water, Catal. Commun., 97 (2017) 125–129.
[35] E.B. Simsek, B. Kilic, M. Asgin, A. Akan, Graphene oxide heterojunction TiO_2-ZnO catalysts with outstanding photocatalytic performance for bisphenol-A, ibuprofen and flurbiprofen, J. Ind. Eng. Chem., 59 (2018) 115–126.
[36] L. Luo, Y. Yang, A. Zhang, M. Wang, Y. Liu, L. Bian, F. Jiang, X. Pan, Hydrothermal synthesis of fluorinated anatase TiO_2/reduced graphene oxide nanocomposites and their photocatalytic degradation of bisphenol A, Appl. Surf. Sci., 353 (2015) 469–479.
[37] W.H.M. Abdelraheem, M.K. Patil, M.N. Nadagouda, Hydrothermal synthesis of photoactive nitrogen- and boron- codoped TiO_2 nanoparticles for the treatment of bisphenol A in wastewater: synthesis, photocatalytic activity, degradation byproducts and reaction pathways, Appl. Catal., B, 241 (2019) 598–611.
[38] X. Zhao, P. Du, Z. Cai, T. Wang, J. Fu, W. Liu, Photocatalysis of bisphenol A by an easy-settling titania/titanate composite: effects of water chemistry factors, degradation pathway and theoretical calculation, Environ. Pollut., 232 (2018) 580–590.
[39] L. Xu, L. Yang, E.M.J. Johansson, Y. Wang, P. Jin, Photocatalytic activity and mechanism of bisphenol a removal over TiO_{2-x}/rGO nanocomposite driven by visible light, Chem. Eng. J., 350 (2018) 1043–1055.
[40] T.B. Nguyen, N.P. Huang, R. Doong, Photocatalytic degradation of bisphenol A over a $ZnFe_2O_4$/TiO_2 nanocomposite under visible light, Sci. Total Environ., 646 (2019) 745–756.
[41] M.P. Blanco-Vega, J.L. Guzman-Mar, M. Villanueva, L. Maya-Trevino, L.L. Garza-Tovar, A. Hernandez-Ramirez, L. Hinojosa-Reyes, Photocatalytic elimination of bisphenol A under visible light using Ni-doped TiO_2 synthesized by microwave assisted sol-gel method, Mater. Sci. Semicond. Process., 71 (2017) 275–282.
[42] P.S. Yap, Y.L. Cheah, M. Srinivasan, T. Lim, Bimodal N-doped P_{25}-TiO_2/AC composite: preparation, characterization, physical stability, and synergistic adsorptive-solar photocatalytic removal of sulfamethazine, Appl. Catal., A, 427–428 (2012) 125–136.
[43] Y. Liu, F. Xin, F.M. Wang, S. Luo, X. Yin, Synthesis, characterization, and activities of visible light-driven Bi_2O_3-TiO_2 composite photocatalysts, J. Alloys Compd., 498 (2010) 179–184.
[44] X. Wu, W. Qin, W. He, Thin bismuth oxide films prepared through the sol-gel method as photocatalyst, J. Mol. Catal. A: Chem., 261 (2007) 167–171.
[45] V.L. Chandraboss, J. Kamalakkannan, S. Senthilvelan, Synthesis of activated charcoal supported Bi-doped TiO_2 nanocomposite under solar light irradiation for enhanced photocatalytic activity, Appl. Surf. Sci., 387 (2016) 944–956.
[46] K.S.W. Sing, Reporting physisorption data for gas/solid systems with special reference to the determination of surface area and porosity (Recommendations 1984), Pure Appl. Chem., 57 (1985) 603–619.
[47] K. Li, C. Dong, Y. Zhang, H. Wei, F. Zhao, Q. Wang, Ag–AgBr/$CaWO_4$, composite microsphere as an efficient photocatalyst for degradation of Acid Red 18 under visible light irradiation: affecting factors, kinetics and mechanism, J. Mol. Catal. A: Chem., 394 (2014) 105–113.
[48] U. Alam, M. Fleisch, I. Kretschmer, D. Bahnemann, M. Muneer, One-step hydrothermal synthesis of Bi-TiO_2 nanotube/graphene composites: an efficient photocatalyst for spectacular degradation of organic pollutants under visible light irradiation, Appl. Catal., B, 218 (2017) 758–769.
[49] U. Alam, A. Khan, W. Raza, A. Khan, D. Bahnemann, M. Muneer, Highly efficient Y and V co-doped ZnO photocatalyst with enhanced dye sensitized visible light photocatalytic activity, Catal. Today, 284 (2017) 169–178.
[50] D.P. Subagio, M. Srinivasan, M. Lim, T. Lim, Photocatalytic degradation of bisphenol-A by nitrogen-doped TiO_2 hollow sphere in a vis- LED photoreactor, Appl. Catal., B, 95 (2010) 414–422.
[51] C.S. Guo, M. Ge, L. Liu, G. Gao, Y. Feng, Y. Wang, Directed synthesis of mesoporous TiO_2 microspheres: catalysts and their photocatalysis for bisphenol a degradation, Environ. Sci. Technol., 44 (2010) 419–425.